CXCR6 governs the retention of tissue-resident memory T cells to promote enhanced surveillance and control of ovarian cancer

Ravikumar Muthuswamy[1*], AJ Robert McGray[1], Sebastiano Battaglia[1], Wenjun He[3], Anthony Miliotto[1], Cheryl Eppolito[1] Brian Lichty[4], Protul Shrikant[5,] and Kunle Odunsi[1,2,6*]

[1]Center for Immunotherapy, Roswell Park Comprehensive Cancer Center, Buffalo, NY, USA.

[2]Department of Immunology, Roswell Park Comprehensive Cancer Center, Buffalo, NY, USA.

[3]Department of Biostatistics & Bioinformatics, Roswell Park Comprehensive Cancer Center, Buffalo, NY, USA

[4]McMaster Immunology Research Centre, McMaster University, Hamilton, ON, Canada.

[5]Department of Immunobiology, College of Medicine, University of Arizona, Tucson, AZ, USA.

[6]Department of Gynecologic Oncology, Roswell Park Comprehensive Cancer Center, Buffalo, NY, USA.

***Corresponding Authors:**

Ravikumar Muthuswamy
Roswell Park Comprehensive Cancer Center
Elm and Carlton Streets
Buffalo, NY14263
Telephone: 716-845-1300x2582
Ravikumar.Muthuswamy@roswellpark.org

Kunle Odunsi, MD, PhD
Roswell Park Comprehensive Cancer Center
Elm and Carlton Streets
Buffalo, NY14263
Telephone: 716-845-8376
Kunle.Odunsi@roswellpark.org

Conflict of interest statement: The authors have declared that no conflicts of interest exist.

Abstract

While the beneficial role played by tissue-resident memory T cells (Trm) in tumor control has emerged, the chemotactic mechanisms associated with their localization and retention in the tumor microenvironment (TME) of cancers including ovarian are poorly understood. The current study has identified chemokine receptor CXCR6 as crucial for Trm responses to ovarian cancer by promoting their localization and retention in the ovarian tumor microenvironment. In human ovarian cancer patients, CXCR6 significantly marked $CD8^+$ $CD103^+$ tumor-infiltrating Trm cells. Functional studies in mice revealed high expression of CXCR6 in tumor-specific T cells that reside in tissues, but not by those in circulation. Knockout of CXCR6 in tumor-specific T cells led to a heightened circulatory response in blood, but diminished resident memory cell accumulation in tumors, culminating in poor tumor control. Analysis of Wild type (Wt.) and CXCR6KO (KO) tumor-specific T cells trafficking in recipient mice using bioluminescent imaging revealed that compared to Wt., KO T cells preferentially localized to the spleen, indicating the possibility of reduced retention in tumor tissues. These findings indicate that CXCR6 by mediating increased retention of tumor-specific T cells in the ovarian tumor microenvironment, promotes resident memory T cell-mediated surveillance and control of ovarian cancer.

Introduction:

In ovarian cancer patients, the density and location of $CD8^+$ tumor-infiltrating lymphocytes (TILs) are critical for determining progression-free and overall survival (1-4). However, recent studies indicate that only ~ 10% of ovarian tumor-infiltrating lymphocytes (TILs) are specific for shared antigens or mutated neoantigens(5). Moreover, the phenotype of tumor-specific T cells, rather than simply the sheer number of T cells is a crucial parameter in determining effective cancer immunity (5-8). In this regard, eliciting T cell responses with durable memory attributes in tumors can lead to better clinical outcomes in cancer patients (9-12). Tissue-resident memory (Trm) cells are a unique subset of memory T cells that lose their recirculatory potential and take up residency in peripheral tissues in areas of previous antigen encounter (13-15). This is in contrast to central memory T cells (TCM) that predominantly circulate within secondary lymphoid organs (SLO) and effector memory T cells (TEM), which recirculate mostly in peripheral tissues. Trm cells are considered as an amalgamation of effector memory TEM and TCM as they share features with both subsets, having effector molecules similar to TEM and renewal/longevity potential similar to TCM (16). Owing to their residency in peripheral tissues, they can act as adaptive sentinels capable of inducing rapid and robust antigen recall responses, by eliciting systemic effector functions, without the requirement for priming in the lymph node (17-20). They are metabolically adept to persist and survive longer in peripheral tissues (21). Further, studies in mice and humans indicate their presence in tumors predicts enhanced tumor control and progression-free survival (22-26).

Based on these attributes, Trm cells represent an important T cell subset capable of generating robust anti-tumor immunity, and therapies like adoptive cell transfer and immune checkpoint blockade will greatly benefit from improving their accumulation in tumors (27-29). However, little is known about the factors that govern Trm localization and retention in tumor tissues, one of the critical steps in the generation of Trm responses. Thus, identifying the factors and mechanisms that drive Trm localization and retention has profound therapeutic implications for promoting Trm response in tumors, as there are no strategies currently available to promote Trm response in cancer patients.

Chemokines and chemokine receptors are implicated in mobilization/localization of immune cells to peripheral tissues and generation of memory response (30-34) and yet, there are no studies that directly address if specific chemokine receptors facilitate resident memory response by driving localization or retention of $CD8^+$ T cells in cancerous tissues. Our current study addresses this gap and reveals CXCR6 as the predominant chemokine receptor expressed by Trm $CD8^+$ T cells in human ovarian cancer. Using murine models of ovarian cancer, we demonstrate that CXCR6 marks tumor-specific resident memory T cells, and their presence in tumors is associated with increased survival. The deletion of CXCR6 in tumor-specific $CD8^+$ T cells resulted in reduced retention in tumor tissues and increased $CD8^+$ T cell recirculation to the spleen, culminating in diminished resident memory response and reduced control of ovarian tumors. Although a role for CXCR6 in CD8+ T cell resident memory responses using infectious disease models has been reported (35-37), however, its role in governing Trm responses in tumors has not been investigated. This makes the current study novel and

significant, which shows CXCR6 as critical for Trm retention in tumors and the generation of effective Trm responses against ovarian cancer.

Results:

CXCR6 is a dominant chemokine receptor associated with human tumor resident memory CD8$^+$ T cells.

To characterize the potential chemokine/chemokine receptor axes involved in the localization of tissue-resident memory CD8$^+$ T cells in the ovarian cancer tumor microenvironment (TME), we profiled the expression of the known chemokine receptors in Trm (CD3$^+$CD8$^+$CD103$^+$) vs. non-Trm (CD3$^+$CD8$^+$CD103$^-$) cells obtained from ovarian cancer patient tumors using RT-PCR and flow cytometry. We used CD103 for identifying Trm cells, as it is considered a canonical marker for tissue-resident memory cells and predicts favorable outcome in ovarian cancer patients (38-41). While mRNA expression of most chemokine receptors including Trm associated CXCR3 (42) demonstrated no clear differences between Trm and non-Trm, Trm cells consistently showed significant upregulation of CXCR6 mRNA compared to non-Trm Cells (Fig.1A). CCR7 mRNA showed a reverse trend with more expression in non-Trm cells (Fig.1A). Flow cytometry analysis further confirmed the high expression of CXCR6 protein in CD8$^+$CD103$^+$ Trm cells (Fig. 1B) and although CXCR3 was high in CD103$^+$ Trm cells no significant difference was noted in its expression when compared to non-resident CD8$^+$ T cells. Analysis with confocal microscopy further substantiated the co-expression of CXCR6 and CD103 on CD8$^+$ TILs (Fig.1C) and this is consistent with previous reports (43). Analysis of ovarian cancer patient data from TCGA that were stratified (Suppl. Fig.1A) for high CD8 expression (N=210) showed a very strong correlation between CD103 and CXCR6 mRNA markers (Fig. 1D). Furthermore, survival analysis using TCGA data revealed that the CXCR6 marker to be positively associated with the increased survival of ovarian

cancer patients (Suppl. Fig.1B). Together, our studies in ovarian cancer patients strongly suggest CXCR6 as a marker of Trm cells.

The presence of CXCR6$^+$ CD103$^+$ tumor resident memory cells is associated with enhanced protection in a mouse model of intraperitoneal ovarian cancer.

To directly test whether CXCR6 plays a functional role in the localization and efficacy of tumor resident memory responses, we developed a prophylactic vaccination model using a mouse intraperitoneal ovarian cancer model as previously described (44-46). As OVA expressing IE9-mp1 tumor model is highly aggressive and difficult to treat, (46), priming and subsequent challenge with this tumor model are not possible. Therefore, we chose a prophylactic experimental setup. This model (Fig.2A) utilizes (-/+) adoptive cell transfer (ACT) of naïve OT1 CD8$^+$ T cells into B6 recipient, followed by (-/+) priming with OVA expressing maraba virus (Mrb-OVA) vaccination to activate OT1 cells. This is followed by a challenge with OVA expressing IE9-mp1 tumor 30 days after vaccine/priming. We chose OT1 T cells for adoptive transfer to allow for careful monitoring and tracking of T cell responses as shown in previous studies (18, 20, 47). OVA expressing Maraba virus was utilized as the vaccine as it was shown to induce robust anti-tumor CD8$^+$ T cell responses in our previous study (46). We did the tumor challenge after a thirty-day interval following the Mrb-OVA vaccine/prime. This is to give sufficient time for the effector response to subside and allow memory generation. This increases the probability that anti-tumor immunity following tumor challenge would come from vaccine-induced memory cells. As shown in Figs.2B &C, the combination of ACT and vaccination with Mrb-OVA improved tumor protection compared to individual treatments of ACT or vaccination alone. In mice that were tumor-free for 155 days after

tumor inoculation (Fig. 2D), CXCR6 and CD103 markers were highly expressed in these $CD8^+$TILs. Further characterization of these CD8+ TILS, revealed them to be more of effector memory phenotype based on CD44 and CD62L markers and they were also highly positive for CXCR3, a chemokine receptor involved in trafficking from lymph nodes to peripheral tissues. Therefore the presence of $CD8^+CXCR6^+CD103^+$ effector memory cells in tissues of tumor-free mice is indicative of their likely role in mediating protection against ovarian tumors.

CXCR6 is highly expressed in antigen-specific $CD8^+$ T cells that reside in the tumor, but not those in circulation.

Analysis of endpoint tumors (Tumors harvested from mice that developed progressive peritoneal ascites and had an abdominal circumference ≥ of 10 centimeters) from mice that were treated with OT1+Mrb-OVA showed that CXCR6 expression was seen predominantly in tumor-specific $CD90.1^+$ OT1 (Fig.3A), but less frequently in $CD90.1^-$ $CD8^+$ T cells. Similarly, analysis of endpoint tumors in Mrb-OVA alone treated mice, revealed that the endogenous tumor-specific $CD8^+$ T cells (marked by OVA tetramer staining) showed high CXCR6 expression compared to non-specific (OVA tetramer negative) T cells (Suppl. Fig.2A). When CXCR6 expression was compared between $OT1^+$ $CD8^+$ T cells in tumor, spleen, and lymph node tissues of OT1+Mrb-OVA treated mice that had reached endpoint, only tumor-infiltrating $OT1^+$ T cells showed high CXCR6 expression (Figs.3B and 3C). Analysis of CD103 in $CD90.1^+$ TILs, revealed high expression by $CXCR6^+$ cells, rather than in the $CXCR6^-$ subset (Figs.3C and 3D).

CD44 and CD62L marker-based stratification show that $CD90.1^+$ TILs are predominantly of $CD44^+$ $CD62L^-$ effector memory phenotype, whereas those in lymph

nodes and spleen were more of central memory type (Fig. 3C). The observation that Trm cells resembled more of the effector/effector memory than the central memory phenotype, is in agreement with previous observations (24, 42, 48, 49). Sequential comparison of OT1 $CD8^+$ T cells prior to transfer (Top), 7 days post transfer in recipient blood (Middle) and in endpoint tumors (lower) revealed again that CXCR6 is acquired by T cells only in tumors and marks $CD44^+CD62L^-$ $CD103^+$ tumor resident memory cells, but not circulatory cells (Suppl. Fig.2B).

Analysis of additional Trm markers, namely CD69 and CXCR3 revealed that they were found in both circulatory and resident memory $CD90.1^+$ $CD8^+$ T cells (Fig.3C and Suppl. Fig.2B). Similar findings showing non-selective expression of CD69 on resident and circulatory cells have been reported before (50, 51) and can be attributed to the specific tissue microenvironment and tumor model used in this study. Uniform expression of CXCR3 on both resident memory and circulatory memory cells in murine studies, further supported our observations in human Trm. Unvarying expression of CXCR3 on both the subsets and selective late expression of CXCR6 on resident memory cells suggests that while CXCR3 may direct default peripheral migration of both memory subsets to the tumor, CXCR6 selectively promotes tissue residency of memory cells. The above observations strongly attest to the validity of CXCR6 as a Trm marker with functional implications in resident memory response to ovarian tumors.

$CD103^+$ T cells localize near multiple cell types that express CXCL16 including $F4/80^+$cells.

To further investigate the role of CXCR6 in shaping $CD103^+$ T cell localization in the TME, we examined whether $CD103^+$ T cells were found close to cells expressing

CXCL16, the main identified ligand for CXCR6 (52). We stained for CD3, CD103, and CXCL16 markers in endpoint tumor tissues and analyzed using confocal immunofluorescence microscopy. The analysis revealed that $CD3^+$ $CD103^+$ T cells were found proximal to CXCL16 positive cells (Fig.4A).To identify the cell source of CXCL16 expression in tumors, we stained tissues from endpoint tumors from OT1+Mrb-OVA treated mice with antibodies for mouse CXCL16 and EPCAM (Tumor Cell marker) and CD45 (immune cells). Confocal microscopy analysis revealed that tumor cells (EP-CAM), $CD45^{+,}$ and $CD45^-$ cells all contributed to CXCL16 expression (Suppl. Fig.3). On further analysis, $F4/80^+$ cells were found to be one of the contributors to CXCL16 (Fig.4B) among immune cells. The above observations suggest that there are multiple sources including F4/80+ macrophages that express CXCL16 in the ovarian cancer microenvironment that support the local accumulation of $CXCR6^+$ Trm.

Knockout of CXCR6 in tumor-specific $CD8^+$ T cells enhances circulatory but reduces resident memory response in tumors, leading to diminished protection against ovarian cancer.

To determine if CXCR6 plays a critical functional role in Trm generation and tumor immunity, CXCR6KO OT1 mice were generated by crossing OT1 PL RAGKO mice with CXCR6KO mice. *In vitro* testing confirmed no clear phenotypic or functional differences between Wt. and CXCR6KO OT1 T cells, as no differences were noted in marker expression (Suppl. Fig.4A) or their lytic capacity against IE9-mp1 target cells (Suppl. Fig.4B). ACT of Wild type (Wt.) or CXCR6KO (KO) $CD90.1^+$ OT1 cells into B6 recipient mice ($CD90.2^+$) was performed on Day -31, followed by vaccination with Mrb-OVA at Day -30 and tumor implantation on day 0 (Fig.5A). Blood analysis on Day -23 (7 days after

ACT+ vaccination) revealed the B6 recipients that received the adoptive transfer of KO T cells showed significantly higher circulatory T cell response than those that received Wt. T cells (Fig.5B). This was backed by similar findings in the spleen of B6 recipient mice that received KO T cells, as they again showed a higher percentage of CD90.1$^+$ T cells compared to Wt. recipients (Fig.5C and Suppl. Fig.5). In contrast quantification of TILs in endpoint tumors, revealed that B6 recipients of CD8 T cells from KO mice had few or no detectable CD90.1$^+$ TILs compared to that received from Wt. mice, where CD90.1$^+$ TILs were consistently detected (Fig.5D). This was also true for CD103$^+$ TILs, as they were also at low frequency or undetectable in recipient mice that received knockout compared to Wt.OT1 (Fig.5E). This difference in transferred T cell persistence in tumors was reflected by differences in tumor progression (Fig.5F) and survival (Fig.5G), as B6 recipients of Wt. CD8 T cells controlled tumors significantly better than KO T cell recipients. Together, the observations confirm that loss of CXCR6 reduces resident memory responses and the associated protection against ovarian cancer.

CXCR6KO on tumor-specific CD8$^+$ T cells prevents retention in tumor tissues and results in the increased localization of T cells to the spleen.

To ascertain whether Wt. or KO CD8 T cells demonstrated different expansion/contraction kinetics and/or spatial differences in T cell localization, we utilized *in vivo* analyses of T cells. To allow specific and sensitive *in vivo* trafficking of transferred T cells, Wt. or KO OT1 mice were bred with B6 T-Lux mice(53), which express the firefly luciferase gene under CD2 promoter to generate Wt. or KO OT1 mice with luciferase-expressing T cells. These luciferase-expressing Wt. or KO T cells after adoptive transfer into recipient mice, can be tracked using *in vivo* bioluminescent imaging (BLI). The

experimental setup (Fig.6A) was similar to that shown in Fig.5A, however, B6 albino recipient mice were used to improve imaging sensitivity following infusion of luciferase-expressing OT1 T cells either from Wt. or CXCR6KO donor mice. *In vivo* imaging was done every week starting 3 days after vaccination. Imaged mice were analyzed for total flux with the region of interest (ROI) annotations done separately for spleen and peritoneum, as shown in Fig.6B. The analysis revealed that compared to Wt., KO T cells redistribute more to the spleen and this was highly significant (Figs.6B & 6C, and Suppl. Fig.6). This finding is concordant with the heightened blood /spleen response (Figs.5B and 5C) seen in recipients of KO T cells. Wt. T cells slowly started to show increased localization towards the omental/peritoneal TME following tumor implantation, but this was not statistically significant (Figs.6B & 6C, and Suppl. Fig.6). In conclusion, *in-vivo* tracking of differences in the spatial distribution of Wt. and KO T cells in recipient mice indicated that deletion of CXCR6 directly impacts T cell tissue distribution, with more predilection of KO T cells to the spleen.

Discussion

The underpinning chemotactic mechanisms guiding Trm localization and retention in the tumor microenvironment (TME) and preventing their emigration have not been clearly defined. Several mechanisms including induction by specific subsets of DC, expression of specific transcriptional regulators HOBIT, BLIMP, Runx3, acquisition of integrins, exposure to homeostatic cytokines and inflammatory signals, and improved metabolic fitness have all been implicated in Trm generation and persistence (21, 32, 42, 54-63). However, most studies have utilized infectious models and the relevance of these factors and associated mechanisms for the generation of Trm responses in cancer is less understood. Given the beneficial role of Trm in tumor control and the increasing need to develop strategies to promote Trm response in tumors, understanding how Trm response is generated and maintained in tumors is warranted. Specifically, identifying the chemotactic mechanisms that drive Trm response to tumors, will greatly help in the design of immunotherapeutic strategies to promote Trm in patients tumors, leading to better therapeutic efficacy and clinical outcome. In our current study, we have characterized Trm responses in both human ovarian cancer specimens and mouse models to identify the chemokine receptor CXCR6 as a key factor driving tumor efficacy due to enhanced residency of tumor-specific T cells within the metastatic ovarian cancer tissues. While a role for CXCR6 in $CD8^+$ T cell resident memory responses using infectious disease models (35-37) has been reported, to date, there are no reports on the functional role of CXCR6 in mediating Trm responses to tumors. This is critical as most mechanisms underpinning immunity against infectious agents versus tumor challenge are distinct. To our knowledge, this is the first study to demonstrate the indispensable requirement for

CXCR6 in tumor resident memory responses and the role in mediating ovarian cancer immunity.

Our results suggest that the chemokine receptor CXCR6 is not involved in T cell trafficking to tumors, as that is served by CXCR3 which shows high expression on both resident and circulatory memory T cells. In contrast, CXCR6 serves as a retention factor to keep T cells in ovarian peritoneal metastatic sites, increasing their likelihood of becoming resident memory cells. This is supported by several observations made in the current study. CXCR6 expression is acquired late and occurs *in situ* in the tumor and CXCR6 is highly expressed in tumor-specific T cells that are resident but not by those in circulation. This is further substantiated by fact that CXCR6 is strongly associated with CD103 (a marker of tissue residency), in both human and mouse studies. In our murine model, the association between CXCR6 and CD103 is stronger in non progressing (tumor-free) mice compared to mice with progressing tumors. This can be attributed to tumor progression induced loss of $CD103^+$ resident memory cells, possibly due to downregulation in E-Cadherin by tumor cells (64). This argues for the development of strategies to increase the persistence of resident memory cells in the TME to enhance the efficacy of cancer immunotherapy.

Knockout of CXCR6 in tumor-specific T cells enhances their responses in blood and spleen but reduces their numbers in the tumor; specifically lowering the frequency of $CD103^+$ resident memory cells and resulting in poor tumor control. Although we observed some tumor control even in recipient mice of KO T cells, this might be due to some contributory responses from circulatory memory cells, as reported previously (65). Our T

cell bioluminescent studies uniquely allowed us to compare the spatial distribution of Wt. and KO tumor-specific T cells over time in recipient mice, and indicated that KO T cells showed increased localization to the spleen, suggesting that loss of CXCR6, reduces tumor retention and enhances emigration out of the TME. Interestingly, there were no appreciable differences between the distribution of Wt. and CXCR6KO T cells in the peritoneum and could be attributable to confounding luciferase signals from circulatory memory cells and mesenteric lymph nodes.

Taken together, our collective results indicate a mechanistic model for the role of CXCR6 in Trm generation in tumors (Figure 7): DC/tumor antigen-activated T cells express CXCR3, driving T cell infiltration into the tumor or peripheral tissues. Once in the tumor, *in situ* acquisition of CXCR6 dictates whether T cells will remain localized to the tumor or emigrate from the ovarian peritoneal tissue microenvironment. CXCR6 on tumor-specific T cells then engage with CXCL16 derived from the TME (produced by macrophages or tumor cells themselves) and facilitates T cell retention. The role of CXCR6 in T cell retention is supported by the previous demonstration that the unique DRF motif in CXCR6 makes it more suited for adhesion than chemotaxis to ligand CXCL16 (66) which exists in both transmembrane and soluble forms (67). We further propose that CXCR6 marks pre-Trm, cells that have increased propensity to become $CXCR6^+$ $CD103^+$ Trm cells, as CXCR6 mediated retention may increase the probability of T cell exposure to TGF-β, a cytokine proposed to induce $CD103^+$ and Trm induction (42, 47, 68).

In conclusion, the present study implicates CXCR6 as a critical regulator for residency and persistence of memory CD8 T cell responses in ovarian TME, thereby

increasing enhanced immunosurveillance and control of ovarian cancer. This warrants targeting the CXCL16/CXCR6 axis in future immunotherapeutic strategies to improve treatment outcomes for ovarian cancer patients.

Materials and Methods

Human studies. Tissue samples were collected from patients undergoing primary tumor debulking surgery for ovarian cancer under a protocol approved by the institutional review board (protocol # I215512). For correlative analysis of immune markers and patient survival, a publicly available ovarian cancer TCGA Firehose legacy 2020 mRNA-seq database (n=307) was used.

Mice studies. Wild type (Wt.) C57BL/6, Albino B6 (C57BL6 mice with a homozygous mutation in the tyrosinase gene), and CXCR6KO were all purchased from The Jackson Laboratory (Bar Harbor, ME). OT1 PL RAGKO (Mice that expresses TCR for $OVA_{257-264}$ peptide and has no endogenous $CD4^+$, $CD8^+$, T, and B cells due to knockout in RAG gene) was a kind gift from Dr. Shrikant. T-Lux mice (53): C57BL6 mice expressing firefly luciferase gene under CD2 promoter was a kind gift from Dr. Casey T. Weaver, the University of Alabama at Birmingham. Wt. C57BL/6 and albino B6 mice were expanded by breeding. OT1 PL RAGKO mice were crossed with CXCR6KO to generate OT1 mice that were deficient for CXCR6. T-lux mice were crossed with Wild type or CXCR6KO OT1 mice to generate luciferase-expressing Wild type or CXCR6KO OT1 mice. All the above crossing and expansion was done under breeding protocol 1145M. Experiments involving the above mice were performed as per the 1371M experimental protocol approved by the Institute Animal Care and Use Committee (IACUC). All animals were maintained in the Laboratory Animal Shared Resource under pathogen-free conditions in the Laboratory Animal Resource (LAR) facility located in Roswell Park Comprehensive Cancer Center (RPCCC).

Adoptive Cell transfer. OT1 $CD8^+$ T cells from Wild type or the knockout mice mentioned above were purified from spleens using EasySep™ Mouse CD8+ T Cell Isolation Kit (#19853, STEMCELL Technologies, Vancouver, CA). Isolated $CD90.1^+$ OT1 $CD8^+$ T cells were injected into $CD90.2^+$ C57BL6 recipient mice at a concentration of 10^6 cells/100ul PBS through the retro-orbital route.

Vaccination. Attenuated strain MG1 of Maraba virus (69, 70) expressing full-length ovalbumin (OVA)was manufactured at McMaster University, their titer determined, shipped on dry ice to RPCCC, and stored at − 80 °C before use. They were injected at 10^7 PFU intraperitoneally for use as vaccine/adjuvant to activate OT1 T cells, that were adoptively transferred one day before to C57BL6 mice.

Tumor model. IE9-mp1, a derivative of widely used ID8 mouse ovarian surface epithelial cell line (71) obtained by one passage in mice and genetically engineered to express Ovalbumin(44), was the tumor cell line used for *in vivo* mice study. Cell line was cultured in RPMI-1640 (10-040-CM) + 10% fetal bovine serum (35-010-CV) in presence of 1x penicillin/streptomycin (100 IU /100 ug mL^{-1}, 30-002-CI) at 37^0C, 5% CO2 conditions. All reagents used for cell line culture are from CORNING, Corning, NY. BL6 mice were injected intraperitoneally (I.P.) with 1x 10^7 cells of IE9-mp1. All the control and treated mice were euthanized when their abdominal circumference is ≈10 cm, which was considered as the experimental endpoint.

Real-time qPCR analysis. RNA from tumor and cells were isolated by RNeasy kit (#74106, Qiagen,). cDNA conversion of isolated RNA was done by using isCript™ cDNA synthesis kit (#170889, BIO-RAD). cDNA was quantified by using predesigned KiCqStart

SYBR® Green primers (# KSPQ12012, Sigma Aldrich, sequences of the primers provided in supplementary table-1,) specific for the various human chemokine receptor genes and IQ™ SYBR green reagent (# 170882, BIO-RAD) on CFX96 real-time PCR detection system (BIO-RAD). QPCR data were analyzed on CFX manager 3.1 (BIO-RAD).

Flow cytometry of human and mice samples. Human tumors were minced into small pieces, suspended in RPMI media, homogenized into single-cell suspension using Miltenyi gentleMACs dissociater. The single-cell suspension was passed through a 100micron cell strainer, washed, spun on ficoll to remove debris and dead cells. Tumor-infiltrating lymphocytes (TILs) processed from above were further processed for downward analysis. Mice tumors were similarly processed, except for the ficol step, and were straightaway stained with flow antibodies. Human tumor samples were stained with live/dead dye (Zombie Aqua fixable viability kit, #423102 BioLegend) in PBS, followed by staining with BioLegend antibodies specific for CD3(Pe-Cy7, HIT3a, #300316), CD8(BV421, RPA-T8, #300106), CD103 (Alexa Flour 488, Ber-ACT8, #350208) CCR5 (APC-cy7, J418F1, #359110,) and with BD biosciences antibodies specific for CXCR3 (PE, IC6, #560928), CXCR4(APC,12G5, #560936) CXCR6(BV786, 13B 1E5, #743602) and in FACS buffer. Mice tissue samples were stained with live/dead dye, followed by antibodies specific for CD8(FITC, 53-6.7, #553031), CD90.1 (PE, OX7, 554898), CD103 (A700, M290, 565529) from BD biosciences, CXCR6 (BV421, SAO51D1, #151109), CD44 (APC-Cy7, IM7, #103208), CD62L(BV786, MEL-14, 104440), CD69(PE-Cy7, H1.2F3, #104512), CXCR3 (BV650, CXCR3-173, #126531) from BioLegend. Stained samples were acquired on the BD LSRII flow cytometry system using BD FACSDiva

software. Post-run analyses were done using the FCS Express 7 research edition software (De Novo Software, Pasadena, CA).

Confocal microscopy*.* Human or mouse tissue sections were marked on the edge with ImmEdge pen (H-4000, Vector Labs) and fixed in 4% PFA, 15 minutes. Human and mouse tissues were blocked with 5% human or mouse serum respectively for 1 hour at room temperature (RT). This was followed by Incubation with fluorophore-conjugated (1:100 dilution) or non-conjugated primary antibodies at (1/500 dilution) for 3 hours at RT. Washed 4 times in 1x PBS. To visualize tumor antigens targeted with non-conjugated primary antibodies, fluorophore-conjugated secondary antibodies(1:1000 dilution, Cell signaling technology) were added along with nuclear dye (Hoechst 33422, # H1399, ThermoFisher) for 30 minutes at RT. Washed 4 times in 1x PBS and sections are mounted with coverslips in prolong gold mounting medium. Tissues are analyzed in Leica SP8 DMRE spectral confocal microscope and Image J software was used for post image analysis. The full details of antibodies and secondary antibodies used for confocal staining of human and mouse tissues are given in supplementary table 2.

In vivo Imaging*.* For *in vivo* imaging studies, we used Wt. or CXCR6KO OT1 T Lux mice as donors for OT1 $CD8^+$ T cells that were adoptively transferred into albino B6 mice. 10^6 cells were used for adoptive transfer and transferred cells were tracked once every week starting from ACT till mice reached the endpoint or signal from the T cells became obscured by the growing tumors. Mice were sedated, 150ul of D-Luciferin (30mg/ml) was injected intraperitoneally (I.P.) per mice, incubated for 10minutes and luciferin intensity was measured on the IVIS Spectrum In Vivo Imaging System (Perkin Elmer, Waltham, MA). Images were taken at 1min exposure and analyzed on living image software.

Cytotoxic T lymphocyte induced activated Caspase3/7 assay. 5 x 10^5 Wt. OT1 and CXCR6 OT1 were incubated by itself or with 5 x 10^4 of OVA expressing IE9-mp1 target cell line or OVA non expressing ID8 cell in the presence of 4uM CellEvent™ Caspase-3/7 Green Detection Reagent (#C10423, ThermoFischer Scientific) in triplicates for 24 hours. Caspase-3/7 fluorescence is measured on Biotek Synergy HT microplate plate reader at emission 528nM. Images of the wells with each condition were taken on ZOE™ fluorescent cell imager (BIO-RAD).

Statistical analysis. All statistical analyses involved in the study were performed using GraphPad Prism 8 software. The type of statistic used is described in the figure legends respectively. For all analyses, $P<0.05$ was considered statistically significant. *, **, ***, and **** indicates $P<0.05$, $P<0.01$, $P<0.001$ and $P<0.0001$ respectively. All Data were expressed as Mean ± SEM except in some cases, where box and whisker plots were used. In the box and whisker plots, the horizontal line represents the median and the whiskers connect the highest and lowest observations.

Mice Study approval. All animal experiments were carried out according to protocol guidelines reviewed and approved by the Institute Animal Care and Use Committee (IACUC) of Roswell Park Comprehensive Cancer Center (Buffalo, NY).

Author Contributions:

RM designed and performed the experiments, analyzed results, and wrote the manuscript

AJRM advised, designed, and performed the experiments, reviewed, and corrected the manuscript.

SB and WH did the TCGA and statistical analysis for the current study

BL engineered maraba-OVA viral constructs.

AM processed and analyzed samples for the human study.

CE bred/crossed and generated mouse strains used, wrote mice protocols, reviewed data, and manuscript.

PS advised on the experiments, revised the manuscript.

KO designed, advised experiments, reviewed and corrected the manuscript.

Acknowledgments

We acknowledge the support from grants: NCI SPORE P50CA159981, NIH U24 CA232979, NIH R01 CA158318, NIH U01 CA233085, NCI Cancer Center Support Grant P30 CA016056, NIH/NCI R01CA220297, and NIH/NCI R01CA216426 grants and core facilities: Laboratory animal resource, Flow and confocal core, Translational Imaging Shared Resource for their help with the current study. We acknowledge Dr. Weaver for providing us the T-Lux mice.

References:

1. Zhang L, Conejo-Garcia JR, Katsaros D, Gimotty PA, Massobrio M, Regnani G, et al. Intratumoral T cells, recurrence, and survival in epithelial ovarian cancer. *N Engl J Med.* 2003;348(3):203-13.
2. Sato E, Olson SH, Ahn J, Bundy B, Nishikawa H, Qian F, et al. Intraepithelial CD8+ tumor-infiltrating lymphocytes and a high CD8+/regulatory T cell ratio are associated with favorable prognosis in ovarian cancer. *Proc Natl Acad Sci U S A.* 2005;102(51):18538-43.
3. Hwang WT, Adams SF, Tahirovic E, Hagemann IS, and Coukos G. Prognostic significance of tumor-infiltrating T cells in ovarian cancer: a meta-analysis. *Gynecol Oncol.* 2012;124(2):192-8.
4. Ovarian Tumor Tissue Analysis C, Goode EL, Block MS, Kalli KR, Vierkant RA, Chen W, et al. Dose-Response Association of CD8+ Tumor-Infiltrating Lymphocytes and Survival Time in High-Grade Serous Ovarian Cancer. *JAMA Oncol.* 2017;3(12):e173290.
5. Simoni Y, Becht E, Fehlings M, Loh CY, Koo SL, Teng KWW, et al. Bystander CD8(+) T cells are abundant and phenotypically distinct in human tumour infiltrates. *Nature.* 2018;557(7706):575-9.
6. Duhen T, Duhen R, Montler R, Moses J, Moudgil T, de Miranda NF, et al. Co-expression of CD39 and CD103 identifies tumor-reactive CD8 T cells in human solid tumors. *Nat Commun.* 2018;9(1):2724.
7. Fraietta JA, Lacey SF, Orlando EJ, Pruteanu-Malinici I, Gohil M, Lundh S, et al. Determinants of response and resistance to CD19 chimeric antigen receptor (CAR) T cell therapy of chronic lymphocytic leukemia. *Nat Med.* 2018;24(5):563-71.
8. Scheper W, Kelderman S, Fanchi LF, Linnemann C, Bendle G, de Rooij MAJ, et al. Low and variable tumor reactivity of the intratumoral TCR repertoire in human cancers. *Nat Med.* 2018.

9. Klebanoff CA, Gattinoni L, and Restifo NP. CD8+ T-cell memory in tumor immunology and immunotherapy. *Immunol Rev.* 2006;211:214-24.

10. Gattinoni L, Speiser DE, Lichterfeld M, and Bonini C. T memory stem cells in health and disease. *Nat Med.* 2017;23(1):18-27.

11. Blanc C, Hans S, Tran T, Granier C, Saldman A, Anson M, et al. Targeting Resident Memory T Cells for Cancer Immunotherapy. *Front Immunol.* 2018;9:1722.

12. Park SL, Gebhardt T, and Mackay LK. Tissue-Resident Memory T Cells in Cancer Immunosurveillance. *Trends Immunol.* 2019;40(8):735-47.

13. Masopust D, and Soerens AG. Tissue-Resident T Cells and Other Resident Leukocytes. *Annu Rev Immunol.* 2019.

14. Mueller SN, and Mackay LK. Tissue-resident memory T cells: local specialists in immune defence. *Nat Rev Immunol.* 2016;16(2):79-89.

15. Schenkel JM, and Masopust D. Tissue-resident memory T cells. *Immunity.* 2014;41(6):886-97.

16. Milner JJ, and Goldrath AW. Transcriptional programming of tissue-resident memory CD8(+) T cells. *Curr Opin Immunol.* 2018;51:162-9.

17. Ariotti S, Hogenbirk MA, Dijkgraaf FE, Visser LL, Hoekstra ME, Song JY, et al. T cell memory. Skin-resident memory CD8(+) T cells trigger a state of tissue-wide pathogen alert. *Science.* 2014;346(6205):101-5.

18. Schenkel JM, Fraser KA, Beura LK, Pauken KE, Vezys V, and Masopust D. T cell memory. Resident memory CD8 T cells trigger protective innate and adaptive immune responses. *Science.* 2014;346(6205):98-101.

19. Park SL, Zaid A, Hor JL, Christo SN, Prier JE, Davies B, et al. Local proliferation maintains a stable pool of tissue-resident memory T cells after antiviral recall responses. *Nat Immunol.* 2018;19(2):183-91.

20. Jiang X, Clark RA, Liu L, Wagers AJ, Fuhlbrigge RC, and Kupper TS. Skin infection generates non-migratory memory CD8+ T(RM) cells providing global skin immunity. *Nature.* 2012;483(7388):227-31.

21. Pan Y, Tian T, Park CO, Lofftus SY, Mei S, Liu X, et al. Survival of tissue-resident memory T cells requires exogenous lipid uptake and metabolism. *Nature.* 2017;543(7644):252-6.

22. Park SL, Buzzai A, Rautela J, Hor JL, Hochheiser K, Effern M, et al. Tissue-resident memory CD8(+) T cells promote melanoma-immune equilibrium in skin. *Nature.* 2018.

23. Nizard M, Roussel H, Diniz MO, Karaki S, Tran T, Voron T, et al. Induction of resident memory T cells enhances the efficacy of cancer vaccine. *Nat Commun.* 2017;8:15221.

24. Malik BT, Byrne KT, Vella JL, Zhang P, Shabaneh TB, Steinberg SM, et al. Resident memory T cells in the skin mediate durable immunity to melanoma. *Sci Immunol.* 2017;2(10).

25. Ganesan AP, Clarke J, Wood O, Garrido-Martin EM, Chee SJ, Mellows T, et al. Tissue-resident memory features are linked to the magnitude of cytotoxic T cell responses in human lung cancer. *Nat Immunol.* 2017;18(8):940-50.

26. Galvez-Cancino F, Lopez E, Menares E, Diaz X, Flores C, Caceres P, et al. Vaccination-induced skin-resident memory CD8(+) T cells mediate strong protection against cutaneous melanoma. *Oncoimmunology.* 2018;7(7):e1442163.

27. Clarke J, Panwar B, Madrigal A, Singh D, Gujar R, Wood O, et al. Single-cell transcriptomic analysis of tissue-resident memory T cells in human lung cancer. *J Exp Med.* 2019;216(9):2128-49.

28. Dumauthioz N, Labiano S, and Romero P. Tumor Resident Memory T Cells: New Players in Immune Surveillance and Therapy. *Front Immunol.* 2018;9:2076.

29. Amsen D, van Gisbergen K, Hombrink P, and van Lier RAW. Tissue-resident memory T cells at the center of immunity to solid tumors. *Nat Immunol.* 2018;19(6):538-46.

30. Sallusto F, Lanzavecchia A, and Mackay CR. Chemokines and chemokine receptors in T-cell priming and Th1/Th2-mediated responses. *Immunol Today.* 1998;19(12):568-74.

31. Franciszkiewicz K, Boissonnas A, Boutet M, Combadiere C, and Mami-Chouaib F. Role of chemokines and chemokine receptors in shaping the effector phase of the antitumor immune response. *Cancer Res.* 2012;72(24):6325-32.

32. Mueller SN, Gebhardt T, Carbone FR, and Heath WR. Memory T cell subsets, migration patterns, and tissue residence. *Annu Rev Immunol.* 2013;31:137-61.

33. Zhang Q, and Lakkis FG. Memory T Cell Migration. *Front Immunol.* 2015;6:504.

34. Rahimi RA, and Luster AD. Chemokines: Critical Regulators of Memory T Cell Development, Maintenance, and Function. *Adv Immunol.* 2018;138:71-98.

35. Tse SW, Radtke AJ, Espinosa DA, Cockburn IA, and Zavala F. The chemokine receptor CXCR6 is required for the maintenance of liver memory CD8(+) T cells specific for infectious pathogens. *J Infect Dis.* 2014;210(9):1508-16.

36. Zaid A, Hor JL, Christo SN, Groom JR, Heath WR, Mackay LK, et al. Chemokine Receptor-Dependent Control of Skin Tissue-Resident Memory T Cell Formation. *J Immunol.* 2017;199(7):2451-9.

37. Wein AN, McMaster SR, Takamura S, Dunbar PR, Cartwright EK, Hayward SL, et al. CXCR6 regulates localization of tissue-resident memory CD8 T cells to the airways. *J Exp Med.* 2019.

38. Thome JJ, Yudanin N, Ohmura Y, Kubota M, Grinshpun B, Sathaliyawala T, et al. Spatial map of human T cell compartmentalization and maintenance over decades of life. *Cell.* 2014;159(4):814-28.

39. Thome JJ, and Farber DL. Emerging concepts in tissue-resident T cells: lessons from humans. *Trends Immunol.* 2015;36(7):428-35.

40. Webb JR, Milne K, and Nelson BH. PD-1 and CD103 Are Widely Coexpressed on Prognostically Favorable Intraepithelial CD8 T Cells in Human Ovarian Cancer. *Cancer Immunol Res.* 2015;3(8):926-35.

41. Webb JR, Wick DA, Nielsen JS, Tran E, Milne K, McMurtrie E, et al. Profound elevation of CD8+ T cells expressing the intraepithelial lymphocyte marker CD103 (alphaE/beta7 Integrin) in high-grade serous ovarian cancer. *Gynecol Oncol.* 2010;118(3):228-36.

42. Mackay LK, Rahimpour A, Ma JZ, Collins N, Stock AT, Hafon ML, et al. The developmental pathway for CD103(+)CD8+ tissue-resident memory T cells of skin. *Nat Immunol.* 2013;14(12):1294-301.

43. Wong MT, Ong DE, Lim FS, Teng KW, McGovern N, Narayanan S, et al. A High-Dimensional Atlas of Human T Cell Diversity Reveals Tissue-Specific Trafficking and Cytokine Signatures. *Immunity.* 2016;45(2):442-56.

44. Huang RY, Eppolito C, Lele S, Shrikant P, Matsuzaki J, and Odunsi K. LAG3 and PD1 co-inhibitory molecules collaborate to limit CD8+ T cell signaling and dampen antitumor immunity in a murine ovarian cancer model. *Oncotarget.* 2015;6(29):27359-77.

45. Huang RY, Francois A, McGray AR, Miliotto A, and Odunsi K. Compensatory upregulation of PD-1, LAG-3, and CTLA-4 limits the efficacy of single-agent checkpoint blockade in metastatic ovarian cancer. *Oncoimmunology.* 2017;6(1):e1249561.

46. McGray AJR, Huang RY, Battaglia S, Eppolito C, Miliotto A, Stephenson KB, et al. Oncolytic Maraba virus armed with tumor antigen boosts vaccine priming and reveals diverse therapeutic response patterns when combined with checkpoint blockade in ovarian cancer. *J Immunother Cancer.* 2019;7(1):189.

47. Mackay LK, Wynne-Jones E, Freestone D, Pellicci DG, Mielke LA, Newman DM, et al. T-box Transcription Factors Combine with the Cytokines TGF-beta and IL-15 to Control Tissue-Resident Memory T Cell Fate. *Immunity.* 2015;43(6):1101-11.

48. Gebhardt T, Wakim LM, Eidsmo L, Reading PC, Heath WR, and Carbone FR. Memory T cells in nonlymphoid tissue that provide enhanced local immunity during infection with herpes simplex virus. *Nat Immunol.* 2009;10(5):524-30.

49. Martin MD, and Badovinac VP. Defining Memory CD8 T Cell. *Front Immunol.* 2018;9:2692.

50. Walsh DA, Borges da Silva H, Beura LK, Peng C, Hamilton SE, Masopust D, et al. The Functional Requirement for CD69 in Establishment of Resident Memory CD8(+) T Cells Varies with Tissue Location. *J Immunol.* 2019;203(4):946-55.

51. Steinert EM, Schenkel JM, Fraser KA, Beura LK, Manlove LS, Igyarto BZ, et al. Quantifying Memory CD8 T Cells Reveals Regionalization of Immunosurveillance. *Cell.* 2015;161(4):737-49.

52. Matloubian M, David A, Engel S, Ryan JE, and Cyster JG. A transmembrane CXC chemokine is a ligand for HIV-coreceptor Bonzo. *Nat Immunol.* 2000;1(4):298-304.

53. Chewning JH, Dugger KJ, Chaudhuri TR, Zinn KR, and Weaver CT. Bioluminescence-based visualization of CD4 T cell dynamics using a T lineage-specific luciferase transgenic model. *BMC Immunol.* 2009;10:44.

54. Bourdely P, Anselmi G, Vaivode K, Ramos RN, Missolo-Koussou Y, Hidalgo S, et al. Transcriptional and Functional Analysis of CD1c(+) Human Dendritic Cells Identifies a CD163(+) Subset Priming CD8(+)CD103(+) T Cells. *Immunity.* 2020;53(2):335-52 e8.

55. Shin H, Kumamoto Y, Gopinath S, and Iwasaki A. CD301b+ dendritic cells stimulate tissue-resident memory CD8+ T cells to protect against genital HSV-2. *Nat Commun.* 2016;7:13346.

56. Mackay LK, Minnich M, Kragten NA, Liao Y, Nota B, Seillet C, et al. Hobit and Blimp1 instruct a universal transcriptional program of tissue residency in lymphocytes. *Science.* 2016;352(6284):459-63.

57. Milner JJ, Toma C, Yu B, Zhang K, Omilusik K, Phan AT, et al. Runx3 programs CD8(+) T cell residency in non-lymphoid tissues and tumours. *Nature.* 2017;552(7684):253-7.

58. Szabo PA, Miron M, and Farber DL. Location, location, location: Tissue resident memory T cells in mice and humans. *Sci Immunol.* 2019;4(34).

59. Sheridan BS, Pham QM, Lee YT, Cauley LS, Puddington L, and Lefrancois L. Oral infection drives a distinct population of intestinal resident memory CD8(+) T cells with enhanced protective function. *Immunity.* 2014;40(5):747-57.

60. Skon CN, Lee JY, Anderson KG, Masopust D, Hogquist KA, and Jameson SC. Transcriptional downregulation of S1pr1 is required for the establishment of resident memory CD8+ T cells. *Nat Immunol.* 2013;14(12):1285-93.

61. Bergsbaken T, Bevan MJ, and Fink PJ. Local Inflammatory Cues Regulate Differentiation and Persistence of CD8(+) Tissue-Resident Memory T Cells. *Cell Rep.* 2017;19(1):114-24.

62. Bergsbaken T, and Bevan MJ. Proinflammatory microenvironments within the intestine regulate the differentiation of tissue-resident CD8(+) T cells responding to infection. *Nat Immunol.* 2015;16(4):406-14.

63. Zaid A, Mackay LK, Rahimpour A, Braun A, Veldhoen M, Carbone FR, et al. Persistence of skin-resident memory T cells within an epidermal niche. *Proc Natl Acad Sci U S A.* 2014;111(14):5307-12.

64. Shields BD, Koss B, Taylor EM, Storey AJ, West KL, Byrum SD, et al. Loss of E-Cadherin Inhibits CD103 Antitumor Activity and Reduces Checkpoint Blockade Responsiveness in Melanoma. *Cancer Res.* 2019;79(6):1113-23.

65. Enamorado M, Iborra S, Priego E, Cueto FJ, Quintana JA, Martinez-Cano S, et al. Enhanced anti-tumour immunity requires the interplay between resident and circulating memory CD8+ T cells. *Nat Commun.* 2017;8:16073.

66. Koenen A, Babendreyer A, Schumacher J, Pasqualon T, Schwarz N, Seifert A, et al. The DRF motif of CXCR6 as chemokine receptor adaptation to adhesion. *PLoS One.* 2017;12(3):e0173486.

67. Abel S, Hundhausen C, Mentlein R, Schulte A, Berkhout TA, Broadway N, et al. The transmembrane CXC-chemokine ligand 16 is induced by IFN-gamma and TNF-alpha and shed by the activity of the disintegrin-like metalloproteinase ADAM10. *J Immunol.* 2004;172(10):6362-72.

68. Zhang N, and Bevan MJ. Transforming growth factor-beta signaling controls the formation and maintenance of gut-resident memory T cells by regulating migration and retention. *Immunity.* 2013;39(4):687-96.

69. Pol JG, Zhang L, Bridle BW, Stephenson KB, Resseguier J, Hanson S, et al. Maraba virus as a potent oncolytic vaccine vector. *Mol Ther.* 2014;22(2):420-9.

70. Brun J, McManus D, Lefebvre C, Hu K, Falls T, Atkins H, et al. Identification of genetically modified Maraba virus as an oncolytic rhabdovirus. *Mol Ther.* 2010;18(8):1440-9.

71. Roby KF, Taylor CC, Sweetwood JP, Cheng Y, Pace JL, Tawfik O, et al. Development of a syngeneic mouse model for events related to ovarian cancer. *Carcinogenesis.* 2000;21(4):585-91.

Figure legends:

Figure 1. Chemokine receptor CXCR6 is a bonafide marker of human tumor resident CD8 T cells. (A) $CD8^+$TILs from ovarian cancer patients (N=6) were flow-sorted into $CD103^+$ (Trm) and $CD103^-$ (non-Trm) subsets and real-time RT-QPCR was used to profile the expression of CXC, XC & CX3C (Left) and CC (Right) chemokine receptors. mRNA levels were normalized to HPRT1 and chemokine mRNA levels in $CD103^+$ subset were expressed as fold change over $CD103^-$ subset. Data presented as Mean$\pm$SEM and U.D. denotes undetectable. **(B)** $CD8^+$TILs in human ovarian cancer were flow stained for CD103 and chemokine receptors and presented in the left panel as TSNE plot: 1 representative of similar analysis done in 6 patients and the right panel as Box and whisker plot of % CXCR6 in $CD103^-$ and $CD103^+$ CD8 TILs from 6 ovarian cancer patients.. **(C)** Confocal staining for $CD8^+CD103^+CXCR6^+$ Trm cells in ovarian cancer (Scale bars are at 10μM). **(D)** Spearman's rank correlation between CXCR6 and CD103 markers was done in TCGA ovarian cancer patient database that was stratified for high CD8 expression (N=210). A paired 2 tailed T-test was used in **(**A**)** and **(**B**)** and $P<0.05$ was found significant. *, **, and *** indicates $P<0.05$, $P<0.01$ and $P<0.001$ respectively.

Figure-2. The presence of $CXCR6^+CD103^+$ tumor resident memory cells is associated with increased protection. (A) The experimental schema for adoptive cell transfer of OT1 cells in conjunction with Mrb-OVA vaccination is used to drive immune response against OVA expressing IE9-mp1 tumor cell line. **(B)** Tumor progression and **(C)** survival in mice treated with OT1, Mrb-OVA as single treatments or in combination, NS-nonsignificant. **(D)** Density plots of various markers that were used in phenotype analysis of resident memory CD8 T cells in peritoneal tissues harvested from one representative mice #, that was tumor-free for 155 days after tumor implantation. Log-rank (Mantel-Cox) test was used to calculate the mice survival. Mice are N=10 for OT1+Mrb-OVA and N=5 for control, N=4 for OT1, and Mrb-OVA only groups.

Figure-3. CXCR6 defines tumor-specific resident memory CD8 T cells in Mice models of ovarian cancer. (A). CXCR6 expression in non-tumor (CD90.1$^-$) and tumor-specific (CD90.1$^+$) CD8$^+$ T cells in tumors of mice treated with adoptive cell transfer of CD90.1$^+$ OT1 and Maraba-OVA vaccination (N=5). **(B)** Comparison of CXCR6 expression in CD90.1$^+$ tumor-specific CD8 T cells present in tumor, spleen, and lymph nodes tissues (N=5) and shown as box and whisker plot. **(C)** FACS density plots of CD103 and other memory markers expression in CD90.1 gated CD8 T cells in lymph nodes, spleen, and tumors of one representative OT1+Mrb-OVA treated mice. **(D)** Bar graphs of %CD103 in CXCR6$^-$ and CXCR6$^+$ subsets of OT1 CD8$^+$ T cells in tumors tissues of OT1+Mrb-OVA treated mice (N=5). A two-tailed paired T-test was used to analyze data in **(A)**, **(B),** and **(D),** and P<0.05 was found significant. *, **, and *** indicates P<0.05, P<0.01, and P<0.001 respectively, and the data in bar graphs **(A** & **C)** are Mean+SEM.

Figure-4. CD3$^+$CD103$^+$ T cells are proximal to CXCL16+ cells and F4/80 is one of the major sources of CXCL16. Endpoint tumors from OT1+Mrb-OVA treated mice were stained for nuclei (blue) and CXCL16 (Green) along with either **(A)** CD103 (Red) and CD3 (Grey) or with **(B)** CD11b (Grey), F4/80 (Red). T1 to T5 represent 5 individual mice tumors. Green and red triangles indicate CXCL16$^+$ and CD103$^+$ cells respectively in **(A)** Scale bars are at 10μM for **(A)** and 50μM for **(B).**

Figure-5. CXCR6KO enhances T cell response in blood, but conversely lowers it in tumor tissues and weakens ovarian tumor control in recipient mice. (A) The experimental schema for adoptive cell transfer of Wild (Wt.) or CXCR6KO (KO) OT1 cells in conjunction with Mrb-OVA vaccination in B6 recipient mice. **(B)** % CD90.1$^+$ T cells in day 7 post-vaccination blood of B6 recipient mice that received Wt. or KO OT1 cells, N=15 for each. Comparison of % CD90.1$^+$ T cells in the spleen **(C),** tumor **(D),** CD103$^+$ T cells in the tumor **(E)** at the endpoint, tumor progression **(F)** and survival **(G)** between the 2 groups of B6 mice that received adoptive cell transfer of either Wt. (N=15) or KO (N=13) OT1 cells + Mrb-OVA vaccination. Non paired two-tailed T-test was used to analyze data in **(B)**, **(C), (D),** and **(E),** and P<0.05 was found significant

and data is presented as Mean+SEM. Log-rank (Mantel-Cox) test was used to calculate the survival between mice belonging to Wt. and KO groups in **(G)**. *, **, *** and **** indicates P<0.05, P<0.01, P<0.001 and P<0.0001 respectively.

Figure 6. **CXCR6KO in tumor-specific T cells alters their tissue trafficking with more re-distribution to the spleen. (A)** The experimental schema for adoptive cell transfer of luciferase tagged Wild type (Wt.) or CXCR6KO (KO) OT1 cells in conjunction with Mrb-OVA vaccination in B6 recipient mice. **(B)** The left panel indicates the ROI marking strategy for spleen and peritoneum, the right panel is luciferase images are from one representative B6 recipient mice that received ACT of either Wt. or KO OT1 cells +Mrb-OVA vaccine, Expansion and contraction of Wt. and KO OT1 CD8 T cells were tracked starting from 3 days after ACT + vaccination (Day -31) and followed till 36 days of tumor growth. **(C)** Total flux measurement of Wt. and KO OT1 with ROI marked around the spleen and in peritoneum over the course of the experiment. Data presented as Mean+SEM and N=10 mice per group. A 2-way ANOVA test was used to deduce significance between the groups. *** indicates P<0.001. NS-Non-Significant.

Figure-7. CXCR6 mediated retention promotes resident memory T cell-associated immunosurveillance and control of ovarian cancer. Tumor-specific CD8 T cells generated in lymph nodes use CXCR3 for tumor trafficking, however, tumor *in situ* expression of CXCR6 is needed for retention of circulating T cells to CXCL16 expressing tumor stroma and their increased exposure to TME derived TGF-b to become $CD103^+$ tumor resident memory cells leading to increased tumor surveillance and control. The absence of CXCR6 leads to reduced retention, decreased frequency of resident memory cells, but enhanced recirculation of T cells to the spleen or lymphoid tissues culminating in reduced surveillance and control of the tumor.

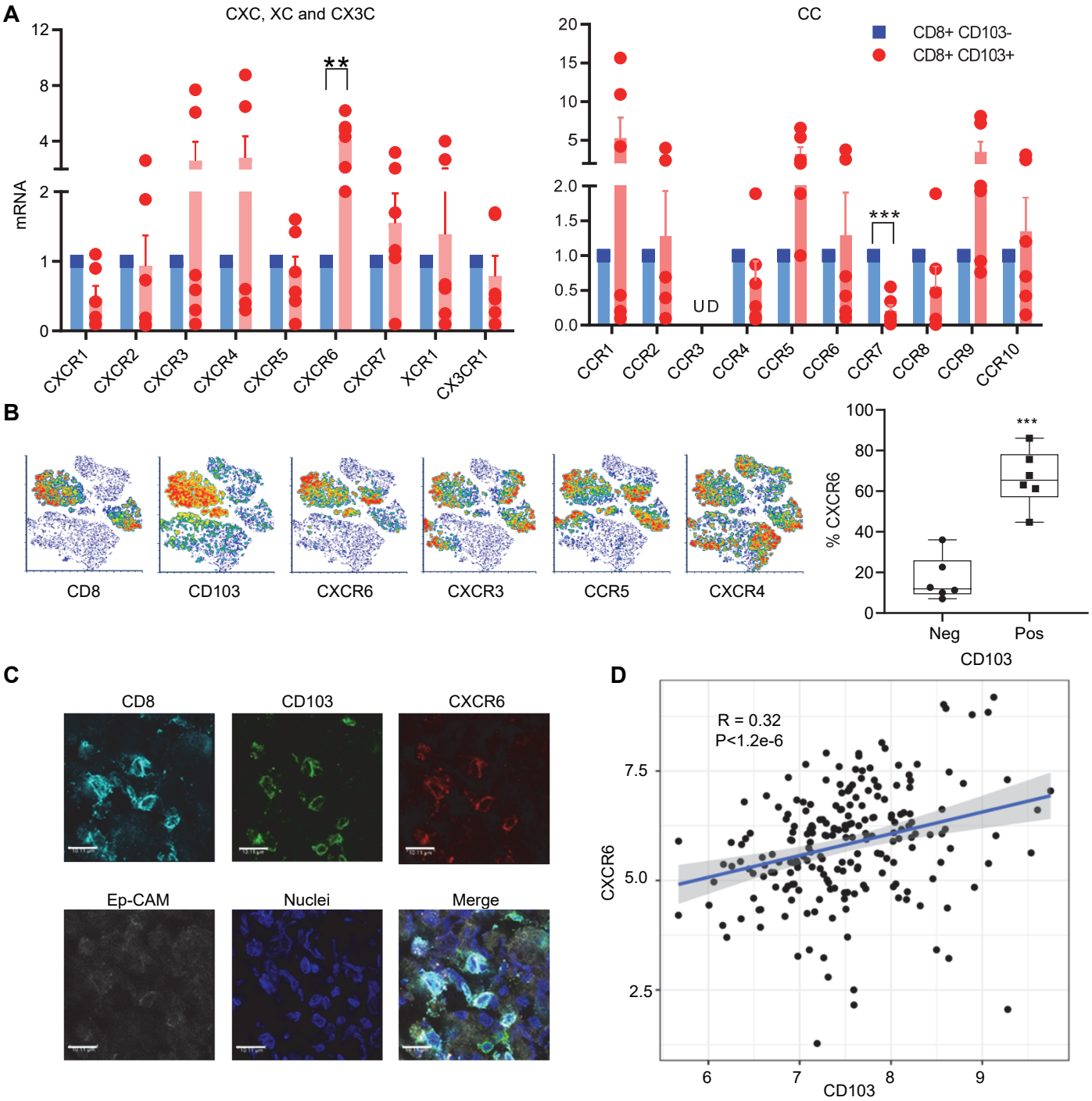

Figure 1. Chemokine receptor CXCR6 is a valid marker of human tumor resident CD8 T cells. (A) CD8$^+$TILs from ovarian cancer patients (N=6) were flow-sorted into CD103$^+$ (Trm) and CD103$^-$ (non-Trm) subsets and real-time RT-QPCR was used to profile the expression of CXC, XC & CX3C (Left) and CC (Right) chemokine receptors. mRNA levels were normalized to HPRT1 and chemokine mRNA levels in CD103$^+$ subset were expressed as fold change over CD103$^-$ subset. Data presented as Mean±SEM and U.D. denotes undetectable. **(B)** CD8 $^+$TILs in human ovarian cancer were flow stained for CD103 and chemokine receptors and presented in the left panel as TSNE plot: 1 representative of similar analysis done in 6 patients and the right panel as Box and whisker plot of % CXCR6 in CD103$^-$ and CD103$^+$ CD8 TILs from 6 ovarian cancer patients.. **(C)** Confocal staining for CD8$^+$CD103$^+$CXCR6$^+$ Trm cells in ovarian cancer (Scale bars are at 10μM). **(D)** Spearman's rank correlation between CXCR6 and CD103 markers was done in TCGA ovarian cancer patient database that was stratified for high CD8 expression (N=210). A paired 2 tailed T-test was used in **(A)** and **(B)** and P<0.05 was found significant. *, **, and *** indicates P<0.05, P<0.01 and P<0.001 respectively.

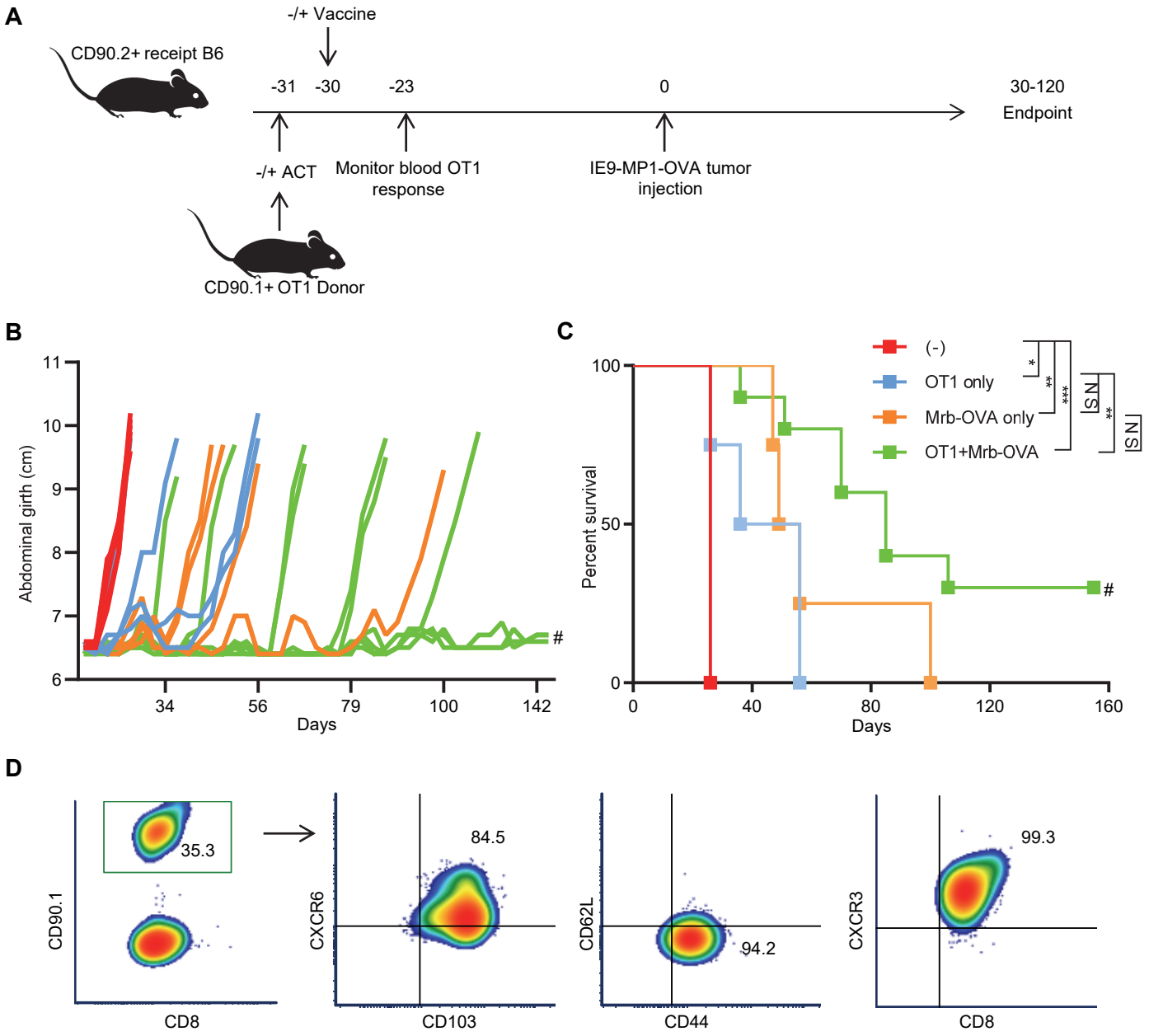

Figure-2. The presence of CXCR6⁺CD103⁺ tumor resident memory cells is associated with increased protection. (A) The experimental schema for adoptive cell transfer of OT1 cells in conjunction with Mrb-OVA vaccination is used to drive immune response against OVA expressing IE9-mp1 tumor cell line. **(B)** Tumor progression and **(C)** Survival in mice treated with OT1, Mrb-OVA as single treatments or in combination, NS-nonsignificant. **(D)** Density plots of various markers that were used in phenotype analysis of resident memory CD8 T cells in peritoneal tissues harvested from one representative mice #, that was tumor-free for 155 days after tumor implantation. Log-rank (Mantel-Cox) test was used to calculate the mice survival. Mice are N=10 for OT1+Mrb-OVA and N=5 for control, N=4 for OT1, and Mrb-OVA only groups.

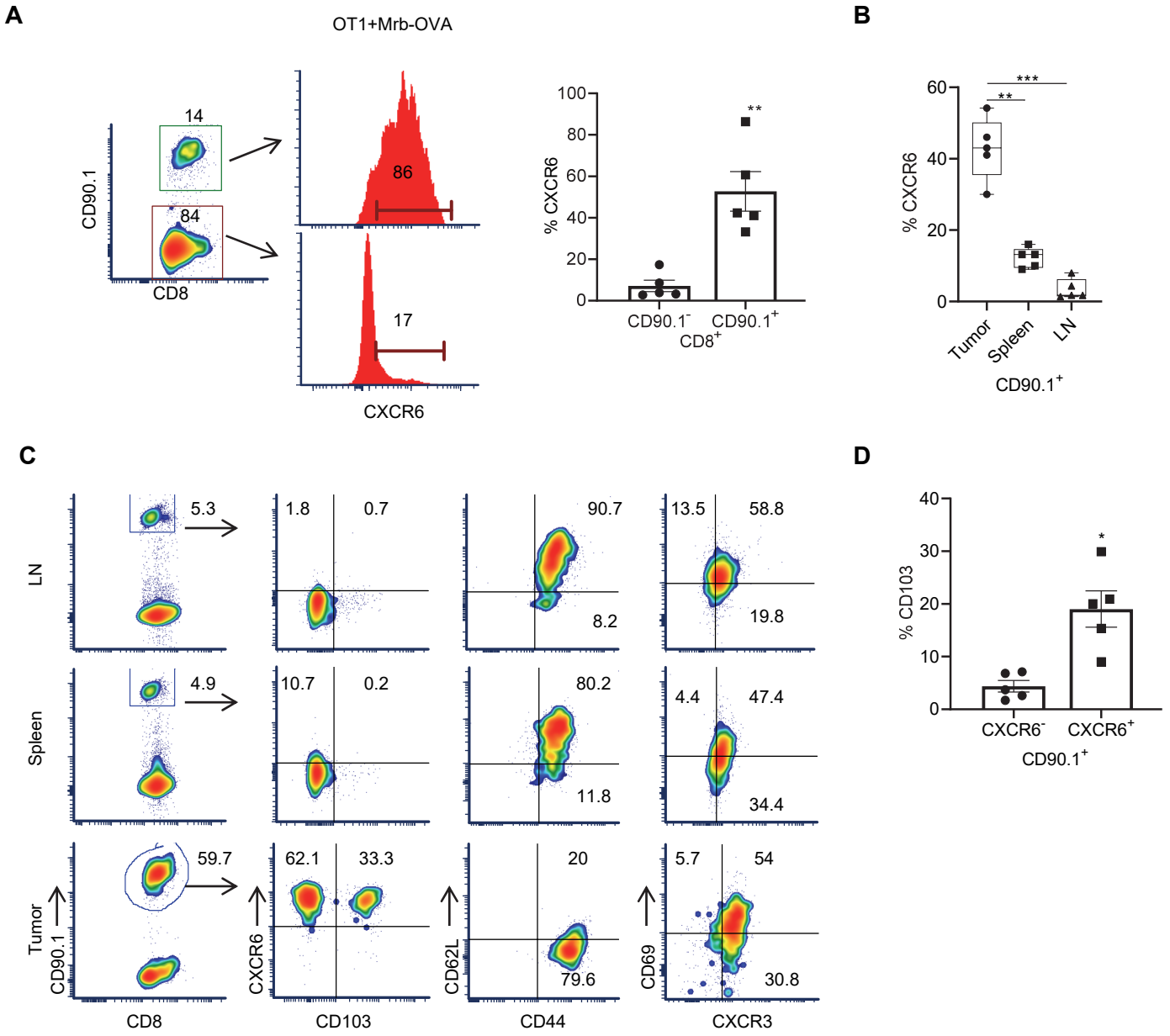

Figure-3. CXCR6 defines tumor-specific resident memory CD8 T cells in Mice models of ovarian cancer. (A). CXCR6 expression in non-tumor (CD90.1⁻) and tumor-specific (CD90.1⁺) CD8⁺ T cells in tumors of mice treated with adoptive cell transfer of CD90.1⁺ OT1 and Maraba-OVA vaccination (N=5). **(B)** Comparison of CXCR6 expression in CD90.1⁺ tumor-specific CD8 T cells present in tumor, spleen, and lymph nodes tissues (N=5) and shown as box and whisker plot. **(C)** FACS density plots of CD103 and other memory markers expression in CD90.1 gated CD8 T cells in lymph nodes, spleen, and tumors of one representative OT1+Mrb-OVA treated mice. **(D)** Bar graphs of %CD103 in CXCR6⁻ and CXCR6⁺ subsets of OT1 CD8⁺ T cells in tumors tissues of OT1+Mrb-OVA treated mice (N=5). A two-tailed paired T-test was used to analyze data in **(A)**, **(B),** and **(D),** and P<0.05 was found significant. *, **, and *** indicates P<0.05, P<0.01, and P<0.001 respectively, and the data in bar graphs **(A** & **C)** are Mean+SEM.

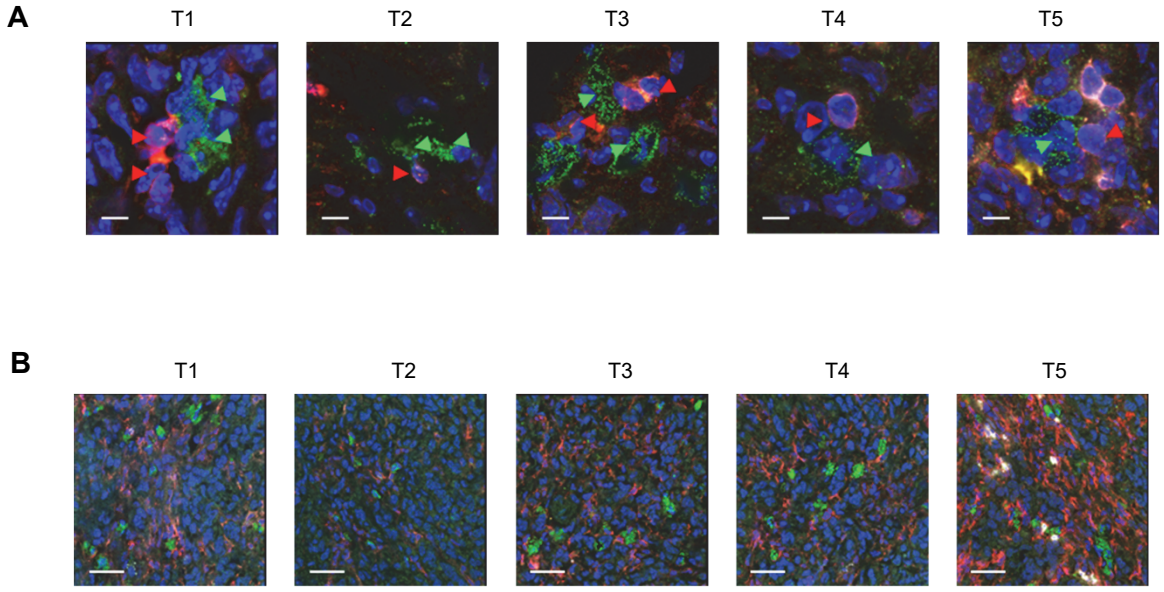

Figure-4. CD3^{+}CD103^{+} T cells are proximal to CXCL16+ cells and F4/80 is one of the major sources of CXCL16. Endpoint tumors from OT1+Mrb-OVA treated mice were stained for nuclei (blue) and CXCL16 (Green) along with either **(A)** CD103 (Red) and CD3 (Grey) or with **(B)** CD11b (Grey), F4/80 (Red). T1 to T5 represent 5 individual mice tumors. Green and red triangles indicate CXCL16^{+} and CD103^{+} cells respectively in **(A)** Scale bars are at 10μM for **(A)** and 50μM for **(B).**

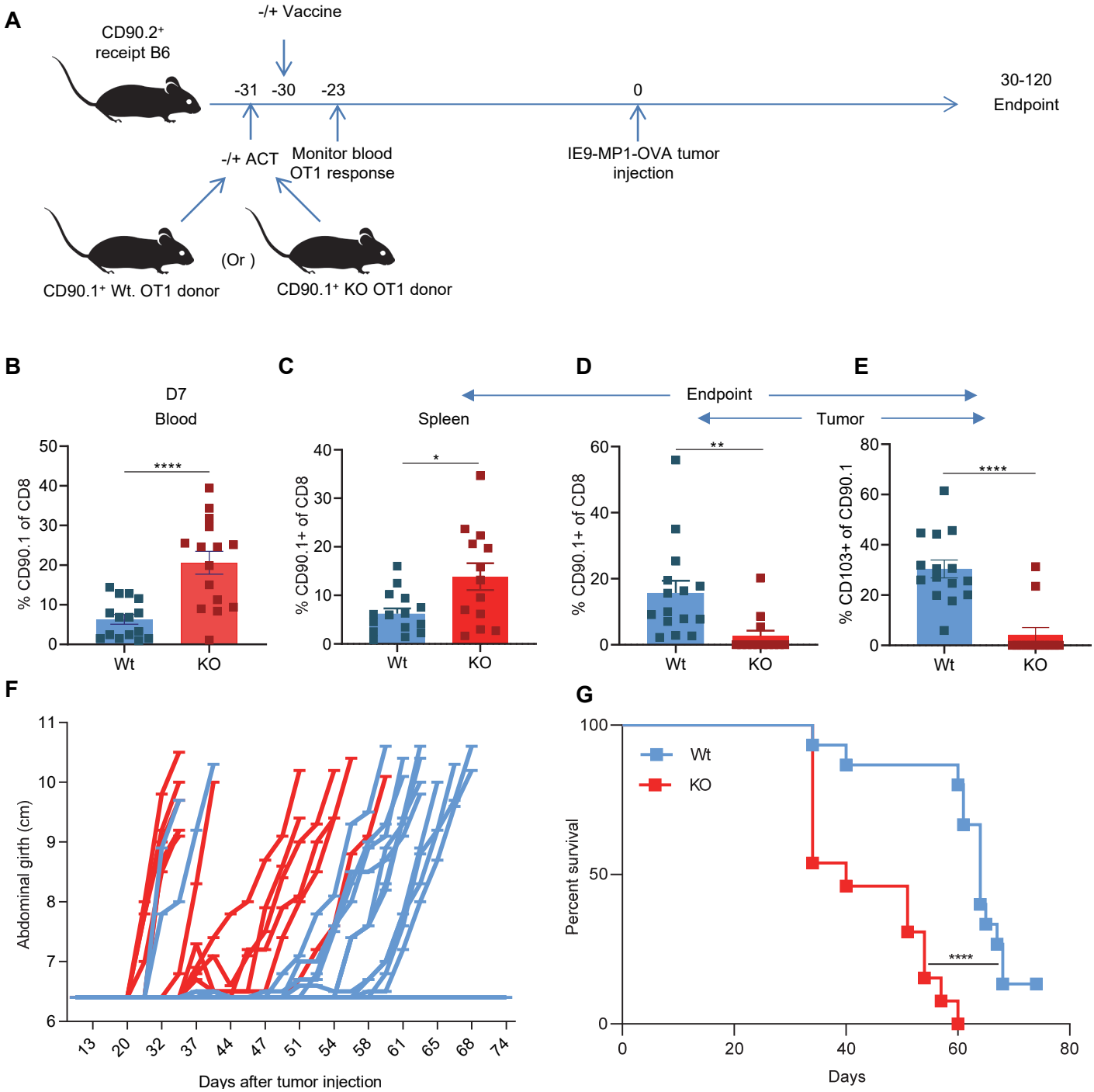

Figure-5. CXCR6KO enhances T cell response in blood, but conversely lowers it in tumor tissues and weakens ovarian tumor control in recipient mice. (A) The experimental schema for adoptive cell transfer of Wild (Wt.) or CXCR6KO (KO) OT1 cells in conjunction with Mrb-OVA vaccination in B6 recipient mice. **(B)** % CD90.1+ T cells in day 7 post-vaccination blood of B6 recipient mice that received Wt. or KO OT1 cells, N=15 for each. Comparison of % CD90.1+ T cells in the spleen **(C),** tumor **(D),** CD103+ T cells in the tumor **(E)** at the endpoint, tumor progression **(F)** and survival **(G)** between the 2 groups of B6 mice that received adoptive cell transfer of either Wt. (N=15) or KO (N=13) OT1 cells + Mrb-OVA vaccination. Non paired two-tailed T-test was used to analyze data in **(B)**, **(C), (D),** and **(E),** and P<0.05 was found significant and data is presented as Mean+SEM. Log-rank (Mantel-Cox) test was used to calculate the survival between mice belonging to Wt. and KO groups in **(G)**. *, **, *** and **** indicates P<0.05, P<0.01, P<0.001 and P<0.0001 respectively.

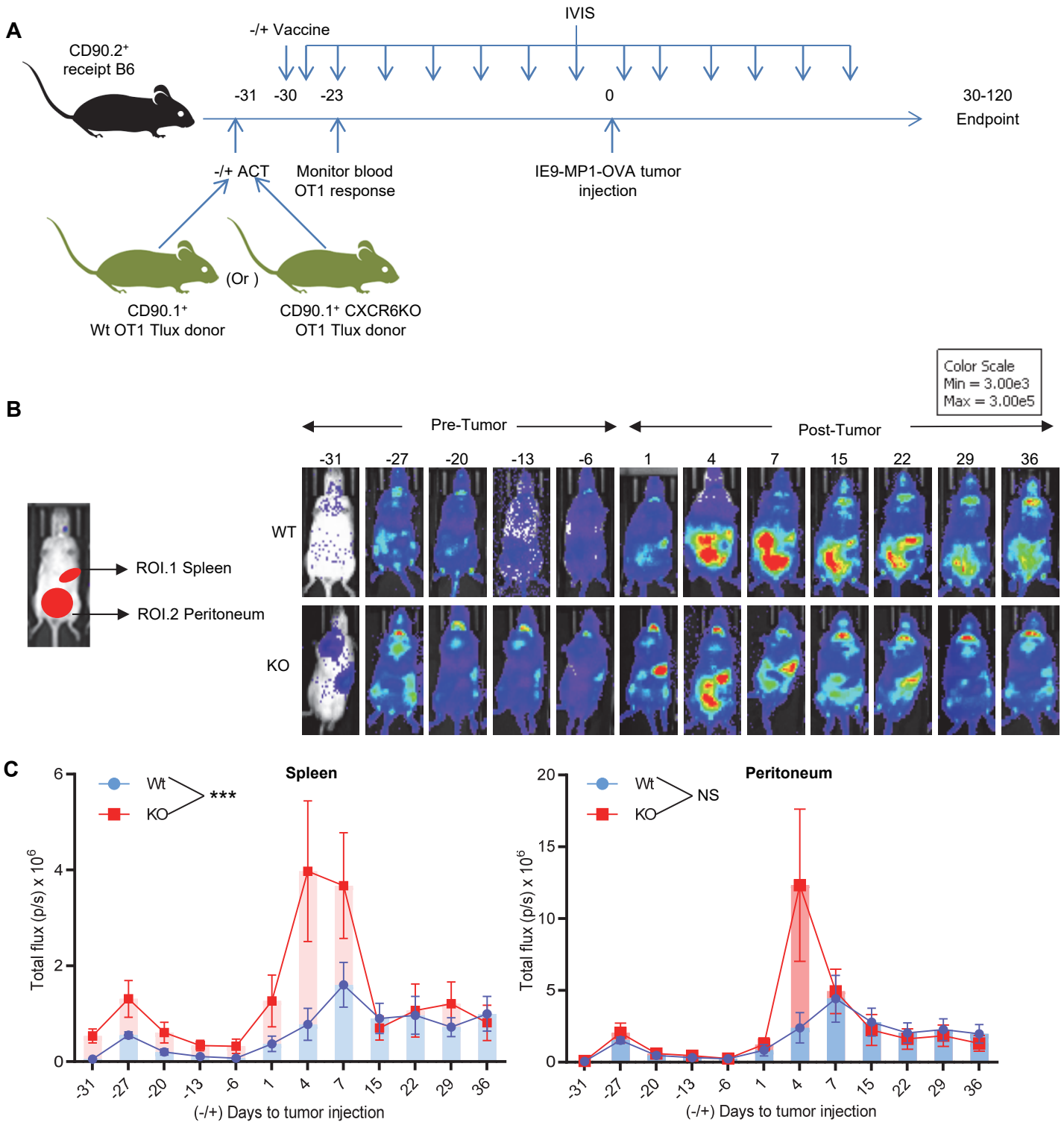

Figure 6. **CXCR6KO in tumor specific T cells alters their tissue trafficking with more re-distribution to spleen. (A)** Experimental schema for adoptive cell transfer of luciferase tagged Wild type (Wt.) or CXCR6KO (KO) OT1 cells in conjunction with Mrb-OVA vaccination in B6 recipient mice. **(B)** Left panel indicates the ROI marking strategy for spleen and peritoneum, right panel is luciferase images are from one representative B6 recipient mice that received ACT of either Wt. or KO OT1 cells +Mrb-OVA vaccine, Expansion and contraction of Wt. and KO OT1 CD8 T cells were tracked starting from 3 days after ACT + vaccination (Day -31) and followed till 36 days of tumor growth. **(C)** Total flux measurement of Wt. and KO OT1 with ROI marked around spleen and in peritoneum over the course of the experiment. Data presented as Mean+SEM and N=10 mice per group. 2-way ANOVA test was used to deduce significance between the groups. *** indicates P<0.001. NS-Non-Significant.

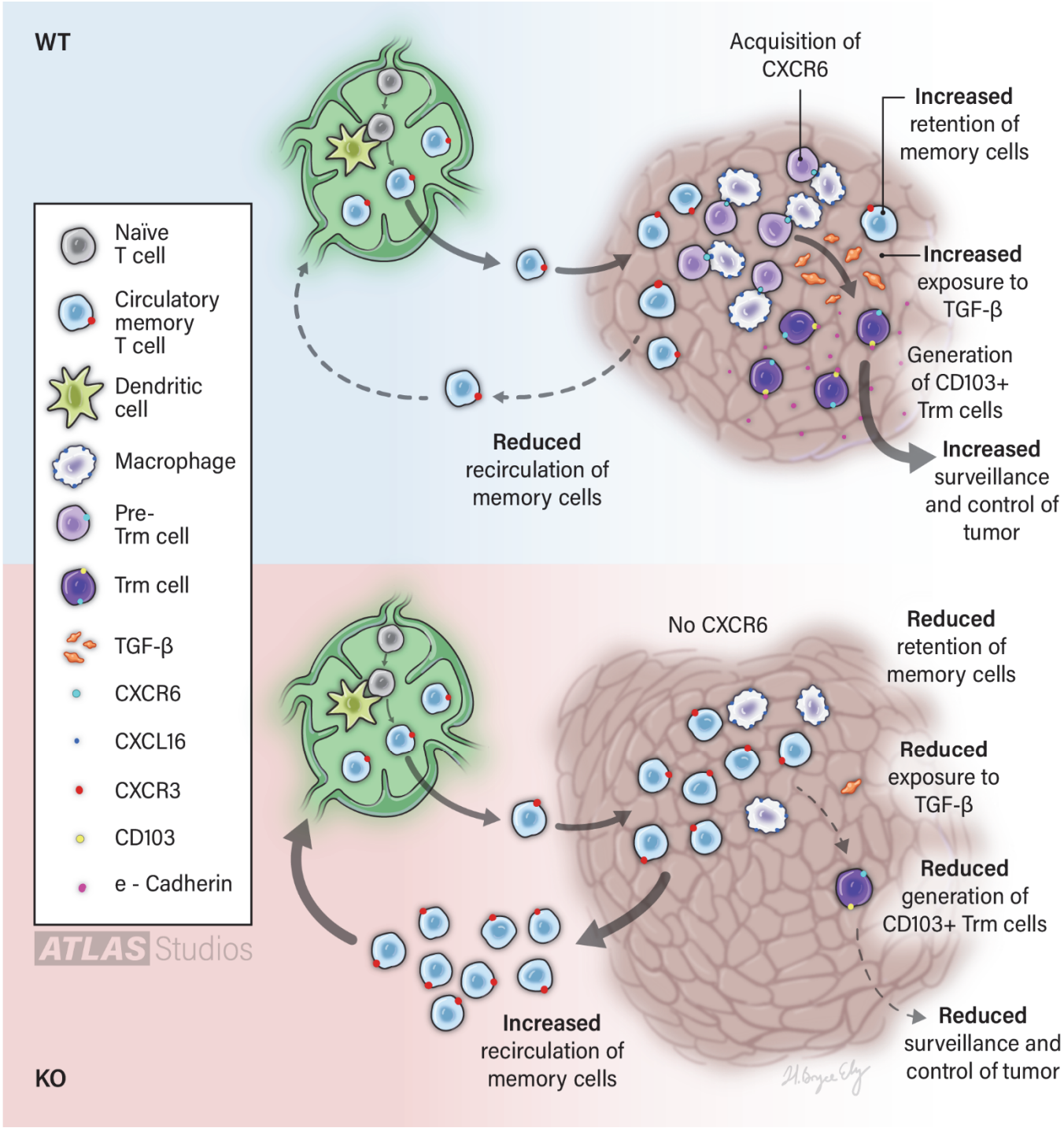

Figure-7. CXCR6 mediated retention promotes resident memory T cell-associated immunosurveillance and control of ovarian cancer. Tumor-specific CD8 T cells generated in lymph nodes use CXCR3 for tumor trafficking, however, tumor *in situ* expression of CXCR6 is needed for retention of circulating T cells to CXCL16 expressing tumor stroma and their increased exposure to TME derived TGF-b to become CD103^{+} tumor resident memory cells leading to increased tumor surveillance and control. The absence of CXCR6 leads to reduced retention, decreased frequency of resident memory cells, but enhanced recirculation of T cells to the spleen or lymphoid tissues culminating in reduced surveillance and control of the tumor.